Honda Research Institute Europe GmbH
https://www.honda-ri.de/

Evolutionary Optimisation of an Exhaust Flow Element with Free Form Deformation

Markus Olhofer, Thomas Bihrer, Stefan Menzel, Michael Fischer, Bernhard Sendhoff

2009

Preprint:

This is an accepted article published in Simulation for Innovative Design, Proceedings of the 4th EASC - 2009 European Automotive Simulation Conference. The final authenticated version is available online at: https://doi.org/[DOI not available]

Evolutionary Optimisation of an Exhaust Flow Element with Free Form Deformation

Markus Olhofer[1], Thomas Bihrer[1], Stefan Menzel[1], Michael Fischer[2] and Bernhard Sendhoff[1]
[1)]Honda Research Institute Europe GmbH, Germany
[2)]Honda R&D Europe GmbH

Abstract
Evolutionary algorithms are well established methods for shape and design optimisations and they are applied to a large variety of problems. Especially for the optimisation of aerodynamic properties various publications demonstrate the potential of the method. Two major problems in the application of evolutionary optimisation methods for the improvement of aerodynamic properties are the representation of the shape and the generation of the CFD mesh necessary for the numerical flow simulations. In this paper a state-of-the-art deformation method named free-form deformation (FFD) is coupled with Evolution Strategies (ES). In this way, both problems are addressed. On the one hand the grid generation for solutions which are generated during the optimisation can be realised. On the other hand a representation of the design is generated, which decouple the complexity of the design to be optimised from the optimisation parameter. In this way it is possible to represent highly complex geometries with a tractable number of optimisation parameter. The combination of ES and FFD is applied to the optimisation of an exhaust flow element for a modern diesel engine. Especially the effects of the representation are demonstrated. Furthermore the problem of solution robustness is addressed in a way that multiple design points are considered during the optimisation in order to generate one optimal solution for a wide range of possible operation conditions.

1. Introduction

Evolutionary algorithms are well established methods for shape and design optimisations and they are applied to a large variety of problems. Especially for the optimisation of aerodynamic properties various publications demonstrate the potential of the method. However, the optimization of three dimensional structures is a very challenging task even today due to several reasons. One factor are the Computational Fluid Dynamics (CFD) calculations which are necessary to evaluate the design at hand. Also from the viewpoint of the optimisation methods several challenging problems are present like the multi-modality of the problem, the fact that gradient information are often not available or too expensive to evaluate and the fact that both, aerodynamic properties and numerical methods, introduce

noise in the quality estimation which hinder the progress of numerical optimisation methods. The effect of these issues become more and more reduced by the progress in the field of CFD simulation, computational speed and by advanced numerical optimisation methods.
However, two other difficult to solve issues hinder very often the numerical optimisation of aerodynamic properties. The first is related to the representation of the geometry which is subject to the optimisation. The other is related to the generation of a computational grid necessary for the evaluation of the design by CFD methods.
The first problem is already addressed by a huge variety of shape representations proposed in the literature, illustrating the high influence on the performance of the optimisation process. One of the difficulties is the trade-off between the high dimensionality of the models which allow a large freedom for shape modifications during the optimisation and a model with a low number of design variables. Whereas a high degree of freedom potentially allows to identify optimal and well tuned solutions, the high dimensionality of the search space often result in a very slow convergence rate of the optimisation method or even in a stagnation at local optima. On the other hand, the restriction to only a few parameters allows for a fast identification of optimal configurations in a low dimensional search space however with the disadvantage of a low flexibility in the representation with the risk of not being able to represent the optimal solution. The majority of representations which are proposed in literature are based on a parameterisation of the surface of a design e.g. by splines with the drawback that complex and involved surfaces result in an extremely high dimensional model with often very involved dependencies between parameter.
An alternative way for the representation is given by deformation approaches in which the deformation of a given base-design is described instead of the geometry itself. In this paper a deformation method named free-form deformation (FFD) is coupled with a numerical optimisation method which is named Evolution Strategy (ES). Free form deformation allows shape modifications by moving the control points arranged in a lattice which encloses arbitrary target geometries. By modifications of the control points of the model, the enclosed design space is deformed independent from the design represented in the space. Therefore the complexity of the design parameter space on which the optimisation algorithm operates is decoupled from the complexity of the design to be optimised.
At the same time it offers a way to realise the CFD grid generation. The computational grid for a modified design can be generated by applying the same deformations to an initial computational grid as for the initial design. Therefore it is often sufficient to generate one single initial grid. A manual update of the grid is afterwards only necessary if deformations are applied which lead to unfavourable local mesh conditions.
In this paper, the combination of FFD with evolutionary optimisation is applied to the optimisation of an exhaust flow element for a modern diesel engine. Since the focus is on the representation of the geometry and the evolutionary optimisation the actual quality calculation including the flow simulation is regarded as black box simulation which returns, after providing a computational grid, the required quality criteria.
The remainder of the paper is structured as follows. After a short description of the applied numerical optimisation method in the next chapter, the deformation method is described in chapter 3. Chapter 4 gives a brief idea about the system the flow element is optimised for. In chapter 5, a description of the encoding of the exhaust flow element, the fitness function, the combination of ES and FFD methods and the setup of the optimisation is given. A description of optimisation results is given in chapter 6, before a conclusion in chapter 7.

2. Evolutionary Algorithms

Evolutionary algorithms (EAs) are direct pseudo-stochastic search methods which mimic the principles of Neo-Darwinian evolution. A population of possible solutions (e.g., a vector of continuous parameters which are also called objective variables in the context of EA) is adapted to solve a given problem (e.g. minimization of pressure drop) over several generations. The adaptation occurs by varying these solutions in the population and by selecting the best solutions for the next generation. The variations can be classified as purely stochastic (usually called mutation) and combinatoric/stochastic (usually called recombination or in the context of genetic algorithms crossover). Schematically the evolution cycle is shown in Figure 1.

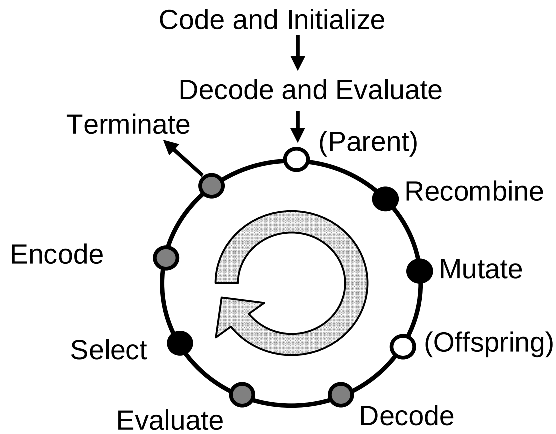

Figure 1: Schematic evolution cycle

In the application presented here, a special variant of Evolutionary Algorithms the so called Evolution Strategy is applied. Standard Evolution Strategies have been described in several textbooks e.g. [1]. Evolution Strategies have been proven to be efficient for the optimisation of continuous parameters due to the utilisation of so called strategy parameter which allow the adaptation of the mutation width along with the object parameter. The effect is a constant adjustment of the algorithm to the current location in the search space.
One of the simplest Evolution Strategies applies only one single strategy parameter which defines the variance of the normal distribution describing the generation of offsprings based on selected parent solutions.
Due to the fact that all parameter are mutated with the same strength the adaptation mechanism in this special Evolution Strategy is called global step size adaptation. This strategy is described in more detail for example in [1].
The mutation operator which is the main source for modifications can be described in this case mathematically by $\vec{x}(t) = \vec{x}(t-1) + N(0,\sigma(t))$. The vector $\vec{x}(t-1)$ describes the parameter set which is subject to the optimization from the former generation and is also called a parent solution. A parameter set for the current generation is generated by adding a realization of a normal distributed random vector with a variance of $\sigma(t)$ where in the most simple case the variance is adapted in a similar way than the object parameter by $\sigma(t+1) = \sigma(t) \cdot \exp(\xi) \quad with\, \xi \sim N(0,\sigma_\xi)$. Here σ_ξ can be regarded as second order adaptation rate. It is usually kept to a constant value depending only on the dimensionality of the problem. The adaptation of the strategy parameter describing the probability distribution for the offspring generation around a parent solution is subject to the main developments and extensions of Evolution Strategies.
In the following, we will conceptually outline the lesser known extensions to Evolution Strategies which have been proposed by Ostermeier [2] and Hansen [3][4] and which have been demonstrated to be very effective both, on benchmark as well as on several practical optimization problems.
Firstly, this is the derandomised strategy which reduces the stochastic influence on the self-adaptation of the strategy parameters. In the original mutative self-adaptation scheme, as

proposed by Schwefel [1] and mentioned above, both the strategy parameters, as well, as the objective parameters are subject to independent stochastic mutations. The idea behind the derandomised strategy is to use one stochastic source for both the adaptation of the objective and of the strategy parameters. In this case, the actual step length (which was used to generate the current successful offspring) in the objective parameter space is used to adapt the strategy parameter, e.g. $\sigma(t)$ in the following way:

$$\sigma(t) = \sigma(t-1)\exp\left(\frac{1}{d}\left(|z| - E\left[\left|N(\vec{0},\vec{1})\right|\right]\right)\right), \quad \text{with } \vec{z} \sim N(\vec{0},\vec{1}) \qquad (1)$$

$N(\vec{0},\vec{1})$ denotes a random vector whose components are Gaussian distributed random variables with zero mean and variance equal to one.

This update rule results in the following, simple, however successful, effect:

If the mutation was larger than expected $\left(|\vec{z}| > E\left[\left|N(\vec{0},\vec{1})\right|\right]\right)$ then the strategy parameter is increased. This ensures that if this larger mutation was successful (i.e. the individual was selected), then such a larger mutation will again occur in the next generation, since $\sigma(t)$ was increased. The same argumentation holds if $\left(|\vec{z}| < E\left[\left|N(\vec{0},\vec{1})\right|\right]\right)$.

Therefore, the self-adaptation of the strategy parameters depends more directly on the local topology of the search space.

The second method is the introduction of the cumulative step size adaptation. Whereas the standard Evolution Strategy extracts the necessary information for the adaptation of the strategy parameters from the population (ensemble approach), the cumulative step size adaptation relies on information collected during successive generations (time averaged approach). This leads to a reduction of the necessary population size. The main idea is to avoid strong correlations (positive or negative) in successive step sizes, because such cumulative steps can be more efficiently realized by single steps.

In the CMA algorithm, the full covariance matrix of the probability density function

$$f(z) = \frac{\sqrt{\det(C^{-1})}}{(2\pi)^{n/2}}\exp(-\frac{1}{2}\left(z^T C^{-1} z\right) \qquad (2)$$

is adapted for the mutation of the objective parameter vector. This has the advantage that the mutation direction is independent from the choice of the coordinate system and correlations between parameters can be represented. If the matrix $\vec{B}$ satisfies $\vec{C} = \vec{B}\vec{B}^T$ and if $\vec{z} \sim N(\vec{0},\vec{1})$ is a Gaussian distributed random variable with zero mean, then an arbitrary normal distribution can be described by $\vec{B}\vec{z} \sim N(\vec{0},\vec{C})$. The adaptation of the objective vector can then be written as:

$\vec{x}(t) = \vec{x}(t-1) + \delta(t-1)\vec{B}(t-1)\vec{z}, \quad \vec{z} \sim N(\vec{0},\vec{1})$, where $\delta(t-1)$ denotes the global step-size of the strategy. Thus, the overall mutation length can be adapted on a faster time scale (one parameter) than the direction which needs the adaptation of the covariance matrix. Since $\vec{C}^{-1}$ has to be positive definite with $\det(\vec{C}^{-1}) > 0$, the different matrix entries cannot be determined independently and the detailed adaptation algorithm combined with the cumulative step-size approach is more involved, see [3][4] for a detailed description.

3. Free Form Deformations (FFD)

Free-Form Deformation (FFD) has been introduced by Sederberg and Parry [5] in the field of computer graphics and computer animation for object manipulation and later extended by Coquillart [6]. Instead of representing the geometry itself, only the deformation of an initial geometry is specified. The initial geometry can be given in any solid modelling scheme. A physical analogy for FFD is to imagine a clear, flexible plastic. The objects which shall be deformed are embedded into the plastic. Deforming the plastic forces the object to change similarly.

The “plastic” is defined by a trivariante Bernstein polynomial consisting of a lattice of control points (CP). To embed an object the coordinates of the object have to be mapped to the coordinates in the spline parameter space, a procedure which is called freezing. If the object is a surface point cloud of the design each point has to be converted into the spline parameter space to allow the deformations. For this calculation various methods have been proposed, e.g. Newton approximation or similar gradient based methods [7].

The deformation of the plastic is realised by changing the position of the control points of the lattice. The object modification is then computed by evaluating a vector valued trivariate Bernstein polynomial. The advantage of representing deformations instead the geometry itself is the decoupling of the representation parameters from the design. Therefore, the number of parameters is independent of the complexity of the shape. It is solely determined by the required flexibility of the deformation.

Deformation methods have been applied to shape optimisation of aerodynamic problems by Perry et al. and Samareh in [8] and together with evolutionary algorithms by Menzel et al. in [13]. It has been shown that FFD methods realize a good trade-off between shape flexibility and a low number of parameter which in turn results in a low dimensional search space for the optimisation.

Furthermore, the representation of deformations enables to modify several objects simultaneously. This also includes the deformation of a grid used in computational fluid dynamics calculations as demonstrated in [8] [9] [13]. Since everything in the control volume is deformed, a grid from computational fluid dynamics that is attached to the shape is also adapted. The new shape and the corresponding CFD grid are generated at the same time without the need for an automated or manual re-meshing procedure even for complex geometries. This feature significantly reduces the computational costs and allows a high degree of automation [12][13][14]. In many cases, design optimisation of complex shapes only becomes feasible when FFD methods are used for the representation.

4. Application

The application to which the optimisation method is applied to is an exhaust gas flow element for a catalytic converter. The task of the element is an increase of the catalytic converter performance by generating an optimal flow distribution of the gas flow in the converter. A schematic description of the overall system is given in Figure 2 assuming a flow direction from right to left.

A simple base geometry was defined initially that consists of 6 blades with a constant wall thickness and a constant radius of curvature. Due to the large variations of possible flow conditions like mass flow and exhaust temperature during normal operation, the design is always a compromise in the sense, that an overall high performance at all possible operation points is necessary rather than a high performance at selected operation points.

For the setup-up the initial configuration, which is referred to as base design in the following, a simulation study was performed to define the optimal radius at selected boundary conditions (i.e. different engine operating points).

The selected geometry was tested on a flow bench to validate the simulation result. Finally it was tested on the engine bench to investigate the improvement of the catalyst activity due to the improved flow distribution. Remarkable improvements were detected for both, the flow profile and the catalyst activity already for the base design.

To further optimize the catalyst performance in the overall system and to reduce the pressure drop at the same time, the numerical optimization of this flow element was performed.

Since the precise evaluation of the catalytic converter performance is very involved a simplified criterion is used in the following with the target to generate a homogeneous flow through the catalytic converter. Therefore two criteria are taken into account for the optimisation. The pressure drop and the homogeneity of the flow through the catalytic converter.

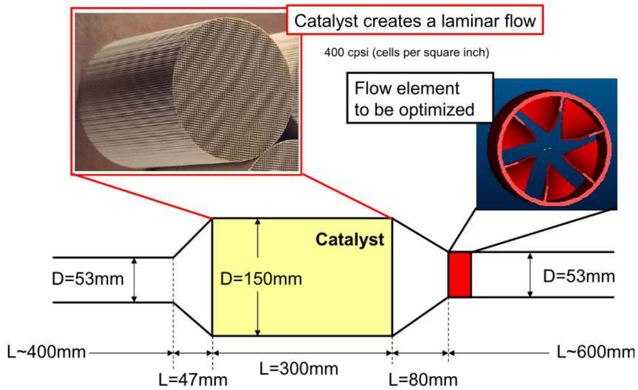

Figure 2: Overall system setup

5. Setup of the Optimization

The initial design of the exhaust flow element is depicted in Figure 3. To represent the rotation symmetric configuration it is transformed in a cylindrical coordinate system.

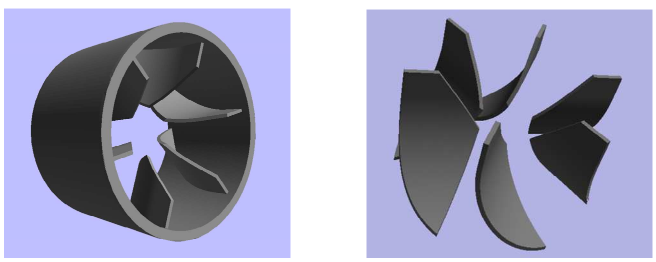

Figure 3: Baseline flow element. (left) including the surrounding wall. Airfoil geometry which was subject to the optimization (right).

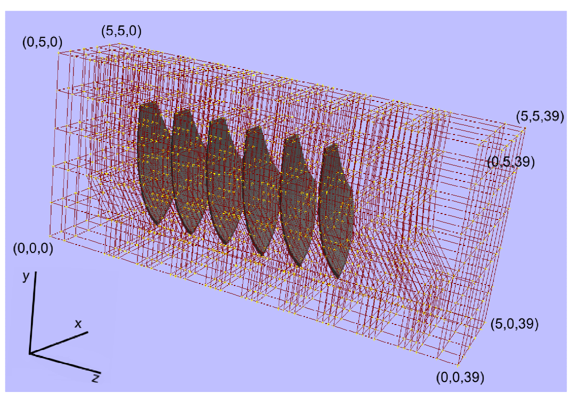

Figure 4: Control volume and flow element in cylindrical coordinate system. Both are scaled in z-direction by factor 100 for visualization.

Figure 4 visualises the control volume which is defined surrounding the configuration. The control volume consists of a lattice of control points. Each blade is contained and therefore controlled by a group of four identical planes of control points in z-direction. In order to simultaneously control all blades this group is repeated 6 times in a distance of $2\pi/6$ units in

z-direction to enclose each single blade. To achieve a uniform deformation of the blades as well as the CFD grid, additional control point planes are added in z-direction in order to generate periodic boundary conditions in z-direction.
In the following, groups of control points are denoted by their indices (indicated in Figure 4) in each direction within the control lattice. Instead of directly modifying the control points a mapping between optimisation parameter and control points is generated which at the one hand allows to simultaneously modify control points which influence corresponding points of the blade and on the other hand to restrict the modifications to areas which have an influence on the blade shape.
In total three optimisation runs are reported in this paper. In the first two optimizations (Run 1 and Run 2) the control grid is modified by five parameters. Each of them specifies the position of a group of control points relative to their initial location. The first parameter effects the control point group (3-4,1-5,2-37) and allow a modification in x-direction. This enables to change the diameter of the outlet in the centre of the tube.
The remaining four parameters change the groups (1-4,1,2-37), (1-4,2,2-37), (1-4,3,2-37) respectively (1-4,4,2-37) in z-direction. In Euclidean coordinates this corresponds to a rotation around the centre of the tube. Thus the slope and outlet angle of the blades can be modified. In the third optimization (Run 3), the limitation on the number of parameter was relaxed by using 17 parameters allowing a higher degree of freedom for modifications. Compared to the representation of Run 1 and Run 2 each of the previously defined four control point groups is divided in four sub groups allowing independent deformations in z-direction which leads to the groups defined by $(i, j, 2-37) \forall i, j = 1...4$. These two sets of parameter define the possible deformations of the flow element and therefore the model for the optimisation.

5.1 Fitness evaluation

The quality of each offspring is evaluated based on CFD simulations and contains two objectives:

1. the pressure loss of the whole exhaust duct,
2. the uniform distribution index 1mm within the catalyst.

Furthermore a penalty for high skewness of the CFD cells is added to the quality measure to avoid unrealistic simulation results. Such cases can occur if the deformation of the CFD grid is large. Moreover, to improve the grid quality before each CFD simulation the smoothing and swapping functions provided by the Fluent software are performed. This reduces the maximal cell volume skewness by about 0.1.

The overall quality function is defined by

$$f(x) = \frac{p(x)}{p_0} - \frac{u(x)}{u_0} + e^{(5s(x)-0.9)} \qquad (3)$$

where $p(x)$ is the pressure loss, p_0 the pressure loss of the base design, $u(x)$ and u_0 the uniform index of the current design and the base design and $s(x)$ the cell equivolume skewness.

In optimization Run 2 and 3 the fitness calculation is based on three different operation points (OP 20, OP 28, OP 66) which differs in the inflow velocity and temperature. The results of the three operation points are weighted according to their expected relevance (40%, 40%, 20%). In optimization 1 only operation point OP28 is evaluated. The CFD simulations were carried out by ANSYS Software Fluent (version 6.3.26). Depending on the operation point the time needed for one calculation is in the range of one to three hours. The overall time for the evaluation of a solution at all three operation points is about 6 hours.

Since all evaluations in one generation are independent from each other the quality evaluations can be done in parallel. In the experiments reported here 10 evaluations are calculated in parallel. This results in a calculation time of one single generation in about 6 hours and an overall calculation time for 56 generations in run 2 of 14 days and of 40 generations in run 3 in 10 days. Since run 1 is evaluated only on one working point the time for the evaluation of one generation is about 2 hours, which results in a calculation time for the experiment of about 2 days.

5.2 Evolution Strategy

In all three optimisation runs a ES-CMA(1,10) was applied, which means that in each generation λ=10 offsprings where generated based on μ=1 selected parent from the previous generation.

6. Results

In this section the results of the three optimization runs are presented. Table 1 and Table 2 summarize calculated performance values for all three working points. In case of Run 1, the performance indices and the fitness are only evaluated for operation point OP28 during the optimisation. The calculated results for Run 1 given in Table 2 at other operation points as well as the fitness given in the second column of Table 1 are calculated afterwards for a comparison of results and were not used during the optimisation.

Table 1: Comparison of performance between Run 1, Run 2 and Run 3

Case	Fitness	Fitness II (OP 28)
Baseline	1.000000	1.000000
Run 1	1.208101	0.967468
Run 2	0.973621	————
Run 3	0.966267	————

Table 2: Comparison between Run 1, Run 2 and Run 3

Case	OP 20	OP 28	OP 66
pressure loss			
Baseline	-835.520	-7375.032	-21047.914
Run 1	-832.938	-7255.462	-20497.779
Run 2	-830.327	-7223.738	-20393.742
Run 3	-828.739	-7197.838	-20259.011
uniformity index 2 (1mm in the catalytic converter)			
Baseline	0.991	0.974	0.959
Run 1	0.995	0.989	0.984
Run 2	0.994	0.984	0.977
Run 3	0.995	0.988	0.985

In case of run 1 the fitness which was achieved during the optimisation is given in a separate third column as Fitness II and is again normalised to the baseline design performance at operation point OP 28 only.

It can be seen that the optimisation which is operating solely on operation point OP 28 increases the quality of the base-design at this operation point. However evaluating the same design with the more realistic quality function integrating other operation points demonstrates that the overall quality (which is a weighted average over three operation points) is decreased to a value of 1.208 and therefore significantly worse than the base-

design. This is a strong indication that the optimisation improved the design quality by reducing the off-design performance. Therefore it seems to be important to optimise the performance of the design simultaneously in the whole range of possible working conditions.
A quality evaluation on 3 different operation points is done in Run 2 by otherwise identical settings to Run 1. It can be seen in Table 1 that the overall quality (fitness) for a realistic working range can be increased by integrating three representative working points.
The difference between Run 2 and Run 3 is related to the flexibility of the model. Run 3 is realised by identical setting to Run 2 with the exception of a higher flexibility of the model like described in chapter 3 and therefore involves a higher number of optimisation parameter. The possible performance increase due to a higher freedom for the optimisation algorithm is demonstrated in Table 1 as well.
The optimization progress for all three runs is presented in Figure 5. The development of the overall fitness during the optimisation is summarised in the right figure. Here it has to be noted again that the plotted fitness values can be compared only Run 2 and Run 3. In case of Run 1 the normalisation is done to the baseline performance at OP28 only. Therefore the fitness values cannot be compared directly. Comparing Run 2 and Run 3 it can be observed that the increase of model flexibility considerable improves the quality of the final solution, however usually with the disadvantage of a lower progress rate.
In the left part of Figure 5 the development of the global step-size which represents the distribution of the offsprings around a parent solution is shown. In case of Run 2 the value becomes close to zero in generation 56. It can be argued that the optimisation is nearly converged, which means that no further progress can be expect. For Run 1 and Run 3 a further improvement could be possible by continuing the optimisation run which was stopped here due to limitations in the computational recourses.
Figure 6 summarises the progress of the optimisation for both criteria, the pressure loss and the uniformity index.

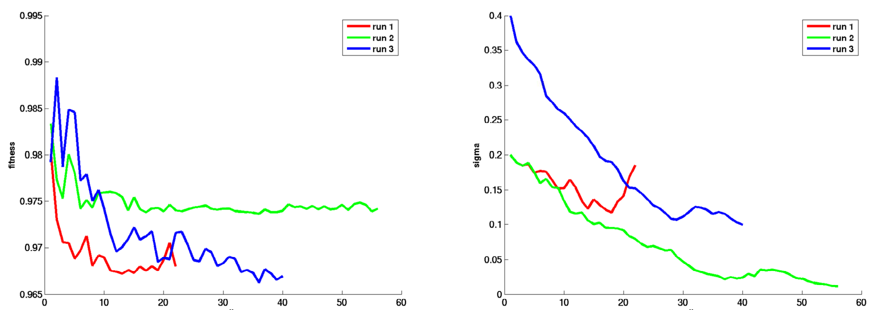

Figure 5: Left: Fitness improvement during the optimization for all three optimization runs. (Please note that the fitness value for run 1 is different because it is based on working point 2 only. Therefore the values cannot directly be compared); Right: Adaptation of the global step-size during the optimization.

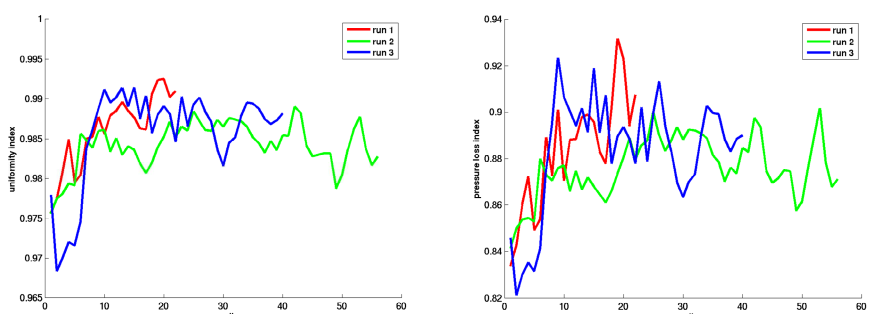

Figure 6: Development of the optimization criteria: Left: uniformity index, Right: pressure loss

Figure 7-9 show the resulting geometries of the best solutions for all three runs compared to the baseline design which is indicated in grey, each in two different views. Comparing the results of run 3 in Figure 9 it can be seen that the higher flexibility of the model is utilised by the optimisation algorithm generating highly bended surfaces.

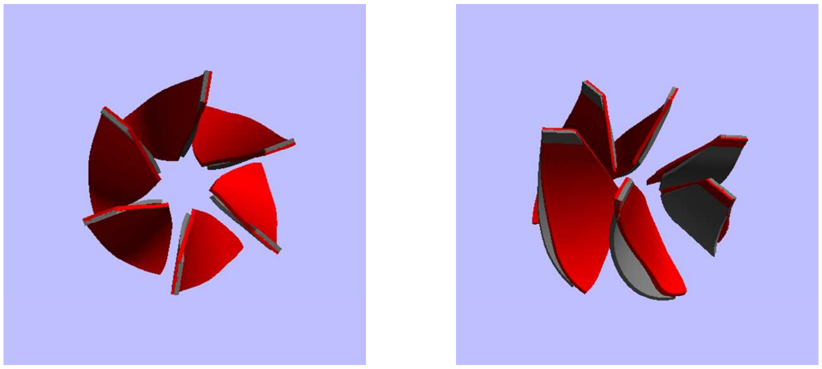

Figure 7: Resulting geometry generated in run1 (red) - compared to baseline (grey)

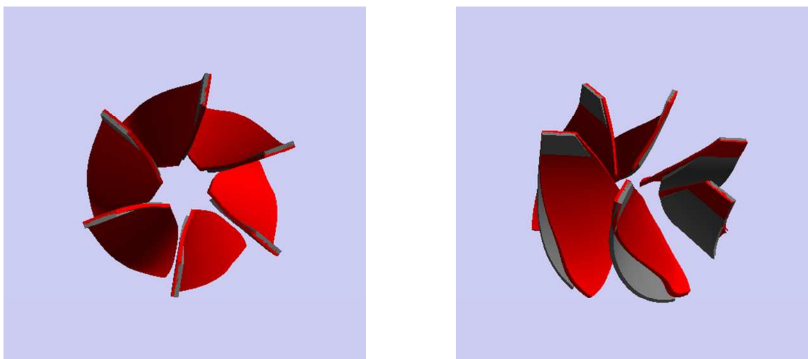

Figure 8: Resulting geometry generated in run 2 (red) - compared to baseline (grey)

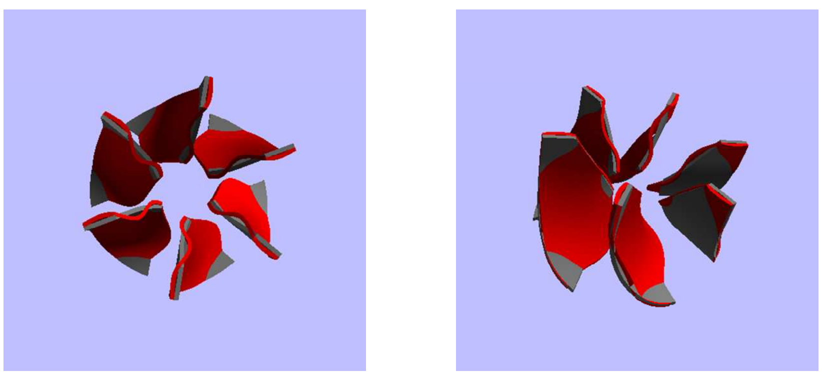

Figure 9: Resulting geometry generated in run 3 (red) - compared to baseline (grey)

The resulting velocity profiles at a cross section 1mm within the catalytic converter is given in Figure 10 for the best optimisation result generated in run 3 and in Figure 11 for the base line design. Here the progress in generating a higher uniformity in the flow velocity can be observed.

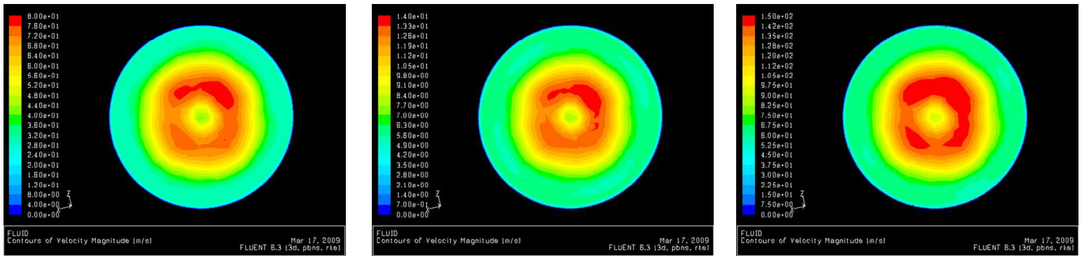

OP20 OP28 OP66

Figure 10: Uniformity Index II for the base-line design for all three operation points

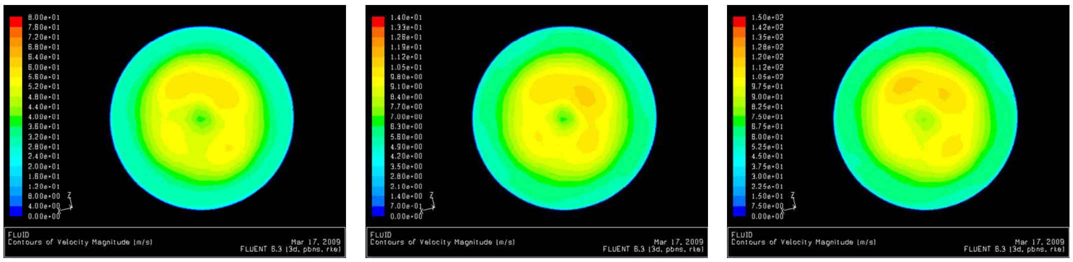

OP20 OP28 OP66

Figure 11: Flow velocity in the catalyst for the optimized design resulting from run 3

7. Summary and Conclusion

The presented results demonstrate the successful application of free form deformation as a well suited representation for the numerical design optimisations. It was demonstrated that a problem representation accessible to numerical optimisation algorithms can be easily created by deformation methods and that a coupling to evolution strategies produces powerful optimisation methods.

A common problem which is known in the application of numerical optimisation methods is the specialisation of results to given design points with the effect of a degeneration of the design performance at off-design conditions. This is problematic for systems which are operated in wide range of possible conditions. Here we address this problem with a very simple method of averaging the results of multiple calculations at different design points within the expected range of working conditions. It can be seen that the average performance of the design can be increased by this method and that robust solutions can be generated which show a high quality in a wide range of working points..

Furthermore the influence of the flexibility of the design model was demonstrated. The differences in the optimisation results between a more restricted model (Run 2) only allowing the modification of selected design areas and a more flexible design model (Run 3) with less restrictions show the expected behaviour. On the one hand the higher freedom for the optimisation results in a higher final quality of the solution. On the other hand the higher number of necessary simulations generates higher overall cost in terms of computational recourses.

Overall it can be seen that the combination of modern optimisation methods, deformation methods and modern flow simulations can generate competitive results even for complex geometries which are otherwise difficult to realise due to problems in the design model generation and also due to problems in the generation of the necessary CFD meshes.

8. Acknowledgements

The authors would like to thank Jörg Böttcher (Honda R&D Europe) for providing the application scenario, support in all questions related to flow conditions of the flow element and defining the quality function. Furthermore the authors would like to thank Hauke Reese from ANSYS Germany GmbH for supporting the optimisation regarding all issues related to the involved CFD simulations and especially for generating and testing the CFD simulation including the quality measures used.

9. References

[1] H.-P. Schwefel, *Evolution and Optimum Seeking*. Wiley, 1995.

[2] A. Ostermeier, A. Gawelczyk, and N. Hansen, *A derandomized approach to self adaptation of evolution strategies*, Evolutionary Computation, vol. 2, no. 4, pp. 369-380, 1994.

[3] N. Hansen and A. Ostermeier, *Adapting arbitrary normal mutation distributions in evolution strategies: The covariance matrix adaptation*, in Proceedings of the 1996 IEEE International Conference on Evolutionary Computation, 1996, pp. 312-317.

[4] N. Hansen and A. Ostermeier, *Completely derandomized self-adaptation in evolution strategies*, Evolutionary Computation, vol. 9, no. 2, pp. 159-195, 2001.

[5] Sederberg, T. W., Parry, S. R., *Free-form deformation of solid geometric models*, SIGGRAPH '86: Proceedings of the 13th annual conference on Computer graphics and interactive techniques, pp. 151--160, 1986

[6] Coquillart, S., *Extended free-form deformation: a sculpturing tool for 3D geometric modeling*, SIGGRAPH '90: Proceedings of the 17th annual conference on Computer graphics and interactive techniques, pp. 187--196, 1990

[7] Piegl, L., Tiller, W., *The NURBS Book*, Springer-Verlag Berlin Heidelberg, 1995 and 1997

[8] Perry, E. C., Benzley, S. E., Landon, M., Johnson, R., *Shape Optimization of Fluid Flow Systems*, ASME FEDSM'00. 2000 ASME Fluids Engineering Summer Conference, Boston, Massachusetts, 2000

[9] Samareh, J. A., *Aerodynamic Shape Optimization Based on Free-Form Deformation*, 10th AIAA/ISSMO Multidisciplinary Analysis and Optimization Conference, 2004

[10] Andreoli, M., Janka, A., Désidéri, J. A., Free-form deformation parameterization for multilevel 3D shape optimization in aerodynamics, Research Report, INRIA, Sophia Antipolis Cedex, France, 2003, 5019

[11] Désidéri, J. A., Janka, A., *Multilevel shape parameterization for aerodynamic opimization - Application to drag and noise reduction of transonic/supersonic business jet*, European Congress on Computational Methods in Applied Sciences and Engineering ECCOMAS 2004, Sophia Antipolis, France, 2004

[12] Menzel, S., Olhofer, M., Sendhoff, B., *Evolutionary Design Optimisation of Complex Systems integrating FLUENT for parallel Flow Evaluation*, Proceedings of the 2nd EACC - European Automotive {CFD} Conference, pp. 279-289, 2005

[13] Menzel, S., Olhofer, M., Sendhoff, B., *Application of Free Form Deformation Techniques in Evolutionary Design Optimisation,* 6th World Congress on Multidisciplinary and Structural Optimisation, Rio de Janeiro, 2005

[14] Perry, E. C., Benzley, S. E., Landon, M., Johnson, R, *Shape Optimization of Fluid Flow Systems,* ASME FEDSM'00. 2000 ASME Fluids Engineering Summer Conference, Boston, Massachusetts, 2000